

# SPIRE STM optical alignment campaign

## Photometer Hartmann test

KD, 11/9/2003

### 1. Reference documents

- RD1 G. Rousset, "HERSCHEL-SPIRE, SPIRE STM MIRRORS, Optical measurement report", LAS.QUA.SPI.PR.V.030024 Iss1 Rev0, 31/03/2003.
- RD2 "Photometer C.S.-tool" drawing SPI-OAL-30-DD-01-A, 07-08--2002.
- RD3 K. Dohlen, "Herschel-SPIRE: Optical error budgets", LOOM.KD.SPIRE.2000.002-4, 17/1/2002.
- RD4 K. Dohlen, "Herschel-SPIRE: Analysis of 3-D measurements of CM3", 15/4/2003.

### 2. Introduction

Measurement of SPIRE image quality is done using a Hartmann test, see Fig. 1. A tool holding a grid of point sources (D-tool) is placed in the position of one of the detectors. A mask containing a grid of holes is placed in the instrument's internal cold stop pupil (Hart tool). A lunette containing two lenses and a CCD camera is placed in front of the instrument entrance (Hartmann lunette). The lunette provides a telecentric image of the D-tool source and the CCD can be placed at different positions before (intra focal) and after (extra focal) the focal plane of the lunette. In extra and intra focal images, distorted images of the Hart tool grid is observed. Determining the position of each point in the grid allows calculation of the wavefront slope, hence quantitative determination of image quality.

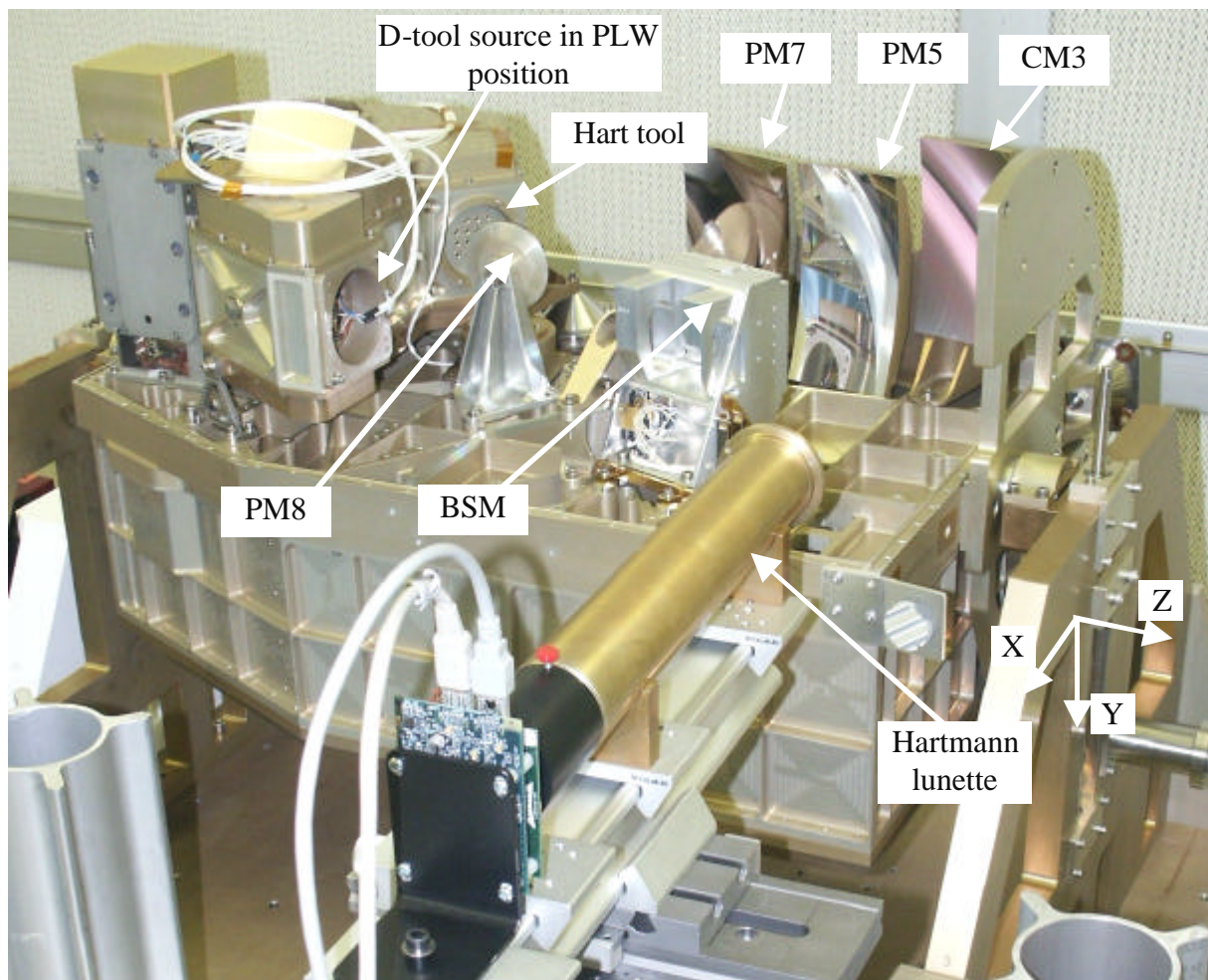


Figure 1. Setup of the Photometer Hartmann test. .

### 3. Coordinate axes

An image was taken of the projection of the PHart tool onto the M2 tool, see Figure 2. To get sufficient intensity, the D tool was replaced with the fiber fed light source. This image allows determination of the axes of the extra and intra focal images, thanks to the left/right asymmetries observed in the pattern of spots, and to the partial shadowing of one of the PHtool holes by the hole in the BSM mirror.

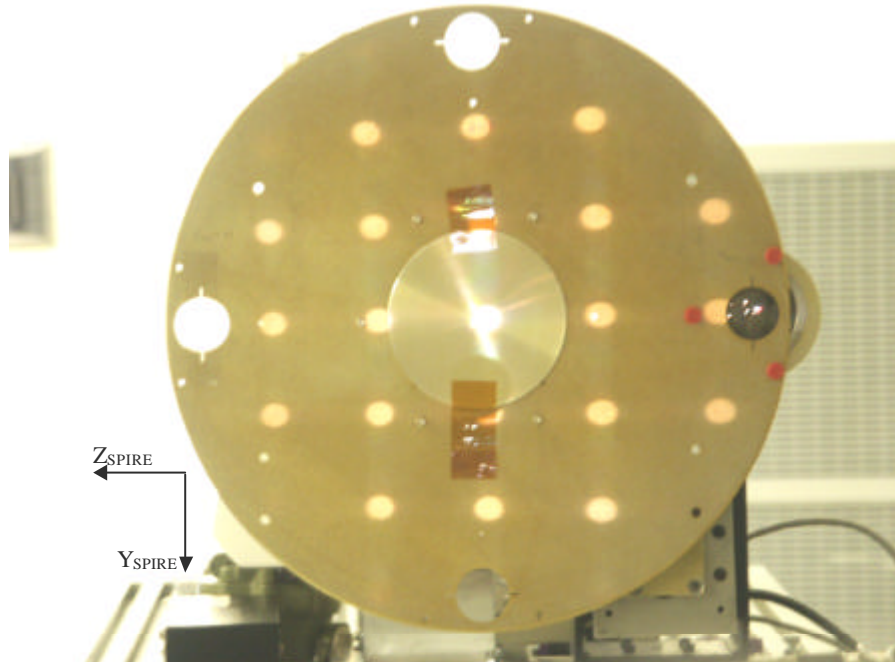


Figure 2. Shadow of the Photometer Hartmann (PHart) tool projected onto the M2 tool. The shadow seen here is obtained after readjustment of the M2 tool so that its centre coincides approximately with the central hole of the PHart tool.. The spot just below the central spot is partly covered by the central hole in the BSM mirror, offset by the insertion of a 4mm shim under its feet.

Figure 3 shows images obtained with the Hartmann lunette for the central D-tool source (a and b), and a comparison of the positions of PHart holes in the M2 plane as estimated from Figure 2 (circles) and as calculated from the slopes deduced from the Hartmann test (dots). Good agreement is found.

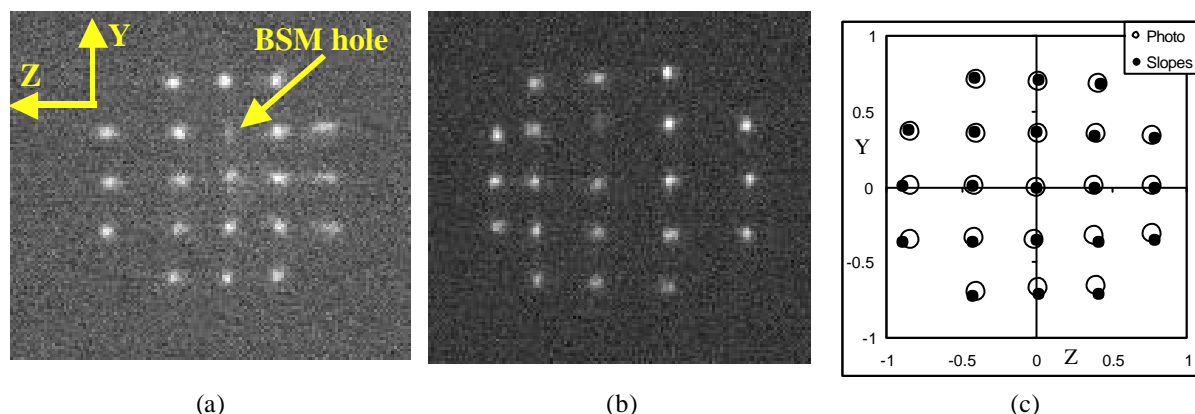


Figure 3. Images obtained with the Hartmann lunette for the central D-tool source (a and b), and a comparison (c) of the positions of PHart holes in the M2 plane as estimated from Figure 2 (circles) and as calculated from the slopes deduced from the Hartmann test (dots).

## 4. Setup and calibration

Before setting up the Hartmann bench in front of the SPIRE camera, it was pointed towards a well-defined object allowing calibration of the detector position on the Hartmann bench. Figure 4 illustrates the parameters involved. The object was placed at the nominal front focal distance (FFD, measured from the front flange of the Hartmann lunette) of  $FFD = 310\text{mm}$ , and the detector slide was adjusted for optimal sharpness of the object (Figure 5). The detector slide position (measured to the back edge of the detector slide) was then  $a+b+c = 472\text{mm}$ . The reference slide was placed such that the distance from its back edge to the detector slide back edge was  $c = 100\text{mm}$ . This distance is measured by the aid of a metallic ruler, and a piece of aluminium added to the reference slide eases this operation. Intra and extra focal distances are measured as deviations from  $c = 100\text{mm}$ . The position of the bench with respect to the instrument is most easily measured from the front edge of the front slide whose position is given by  $a = 49.5\text{mm}$ .

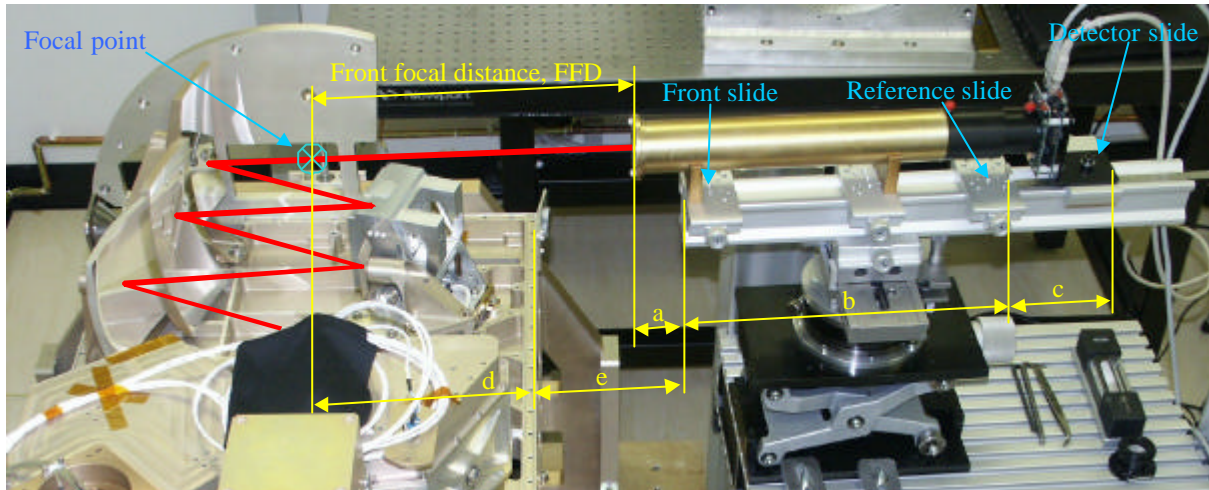


Figure 4. Parameters involved in the axial alignment of the Hartmann bench.

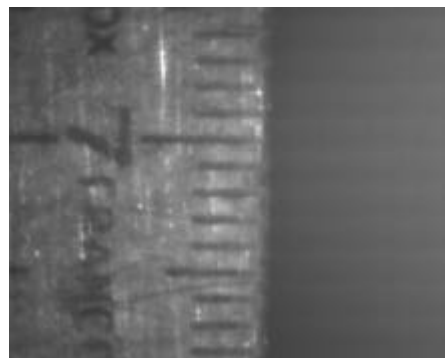


Figure 5. Image of the reference object used for focus calibration of the Hartmann bench.

The Hartmann bench was then turned towards the instrument as seen in Figure 4. Transverse alignment with the gut ray was done using the MAT. Axial alignment was done by measuring by the aid of a ruler the distance  $e$  from the edge of the SOB to the edge of the front slide of the Hartmann bench. Care was taken to measure this distance along the direction of, and directly below, the gut ray. The value of  $e$  was obtained as:

$$e = FFD + a - d$$

where  $d = 1.00415 d_C$  and  $d_C = 215.43$  is the position of the focus in the instrument at 4K, determined by raytracing (Figure 6). Hence  $e = 310 + 49.5 - 1.00415 * 215.43 = 143.18$ .

Due to some erroneous inputs, the value of  $e$  assumed during the tests was 143.8. The precision of the adjustment was estimated to  $\pm 0.5\text{mm}$ .

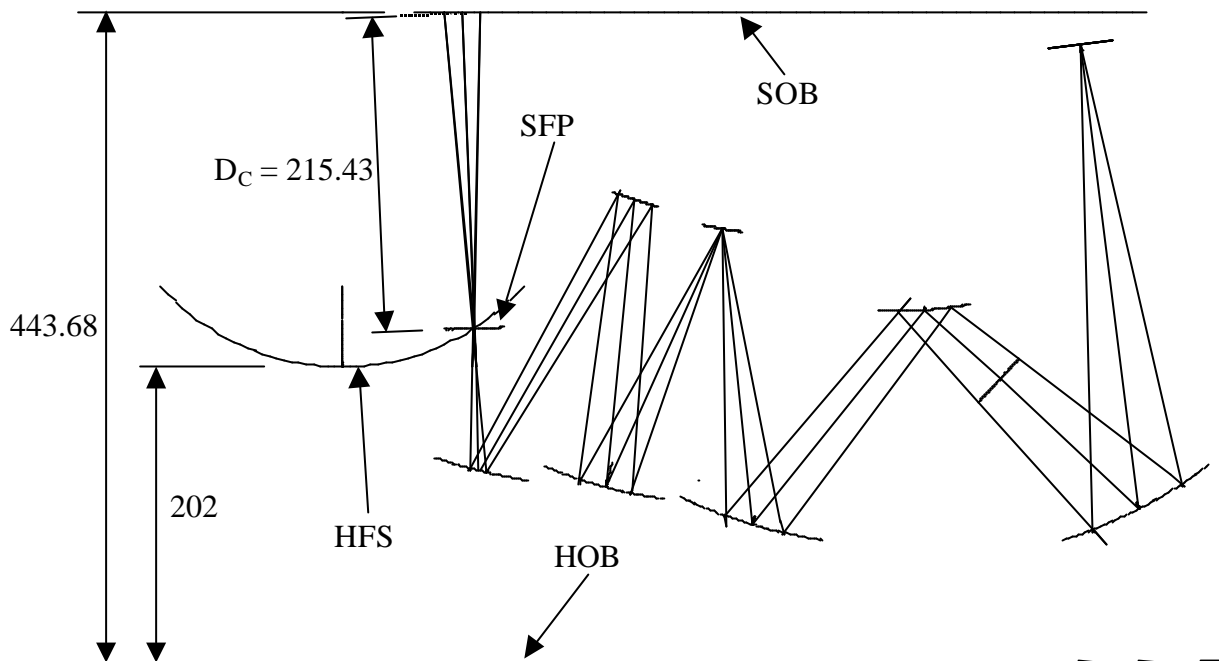


Figure 6. Raytrace model (BolPhtRev25) used to determine the position of the focal plane with respect to the upper edge of the SOB. All dimensions are cold (4K). HOB: Herschel optical bench, SOB: upper edge of the Spire optical bench, HFS: Herschel focal surface, SFP: Spire focal plane, perpendicular to the gut ray at the best focus of the centre of the photometer field.

Lateral alignment to the gut ray using the MAT assures pointing towards the central LED in the D-tool (E). In order to point towards the other LEDs, located in the four corners and named A, B, C, D, lateral shifts and tilts of the Hartmann bench are effectuated. Figure 7 shows a view of the instrument where the field points are defined as projected onto the instrument input plane. Table 1 indicates the adjustments to be done to the Hartmann bench, calculated from outputs from the raytracing model (BolPht155d). Figure 8 defines the Hartmann bench adjustment parameters.

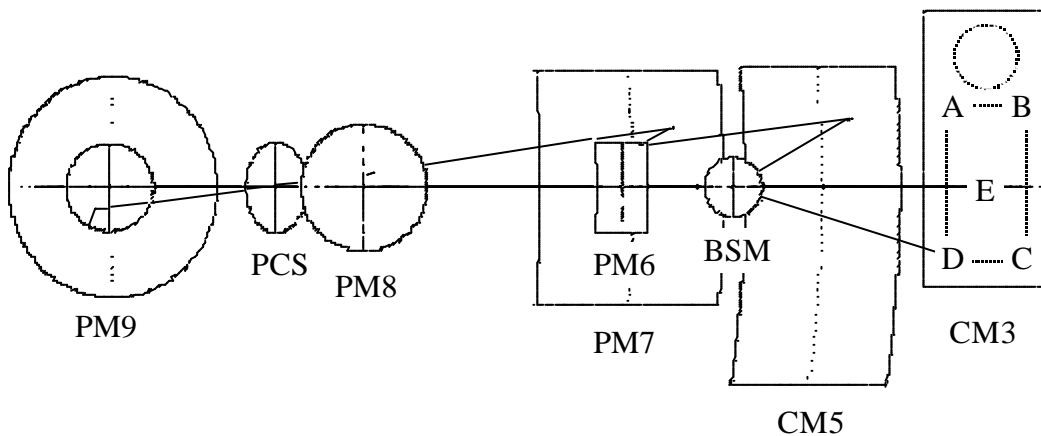


Figure 7. Definition of field points as projected onto the SPIRE input plane.

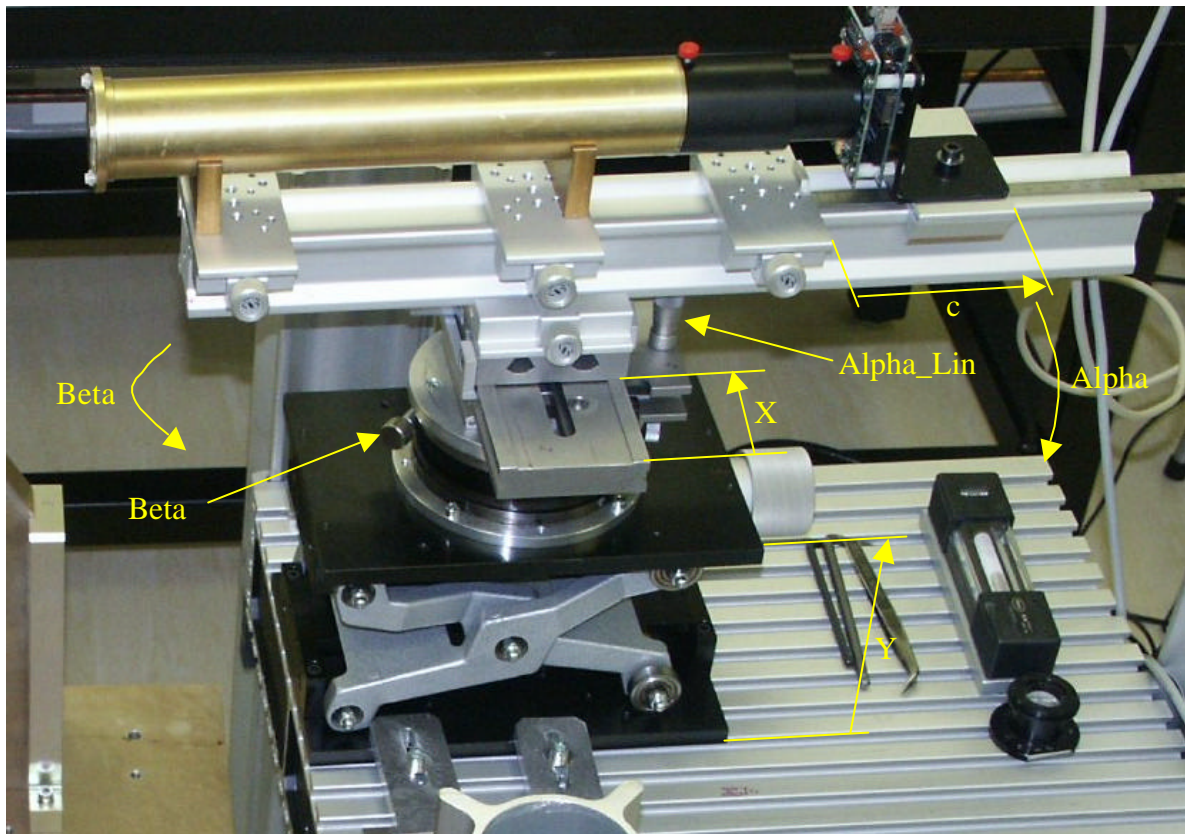


Figure 8. Definition of Hartmann bench adjustment parameters.

Table 1. Calculation of Hartmann bench adjustment parameters for each field point.

<b>Parameter</b>	<b>Unit</b>	<b>E</b>	<b>A</b>	<b>B</b>	<b>C</b>	<b>D</b>
<i>Synopsis input</i>						
H	arcmin	0.00	-2.00	2.00	2.00	-2.00
G	arcmin	0.00	-4.00	-4.00	4.00	4.00
<i>Synopsis output</i>						
tan_beta		0.000000	-0.006301	0.006286	0.006286	-0.006301
tan_alpha		0.000000	-0.012575	-0.012573	0.012573	0.012575
<i>Linear Hartmann bench coordinates</i>						
deltaX	mm	0.00	-12.99	12.96	12.96	-12.99
deltaY	mm	0.00	-25.92	-25.91	25.91	25.92
<i>Angular Hartmann bench coordinates</i>						
deltaBeta_dms	deg:min:sec	-0:0:0	-0:21:40	0:21:37	0:21:37	-0:21:40
deltaAlpha_dms	deg:min:sec	-0:0:0	-0:43:14	-0:43:13	0:43:13	0:43:14
<i>Linear Hartmann bench adjustments</i>						
X	mm	<b>69.50</b>	<b>56.51</b>	<b>82.46</b>	<b>82.46</b>	<b>56.51</b>
Y	mm	<b>142.00</b>	<b>167.92</b>	<b>167.91</b>	<b>116.09</b>	<b>116.08</b>
<i>Angular Hartmann bench adjustments</i>						
Beta_dms	deg:min:sec	<b>130:30:0</b>	<b>130:8:20</b>	<b>130:51:37</b>	<b>130:51:37</b>	<b>130:8:20</b>
Alpha_lin	mm	<b>4.08</b>	<b>5.35</b>	<b>5.34</b>	<b>2.83</b>	<b>2.83</b>

## 5. Data collection and reduction

Once set up for a given point in the field, corresponding to a LED in the D-tool, sliding the detector slide along the rail allows study of the evolution of the Hartmann grid during the passage through focus. Intra and extra focal images are normally taken at defocus distances of  $\pm 15\text{mm}$ , ie at  $c_{\text{Intra}} = 85\text{mm}$  and  $c_{\text{Extra}} = 115\text{mm}$ . In case of excessive aberrations this can be increased. Images are saved as BMP files.

### 5.1. Detect and sort Hartmann points

An IDL program (HartApplic.pro, HartEvent.pro, HarTest.pro) is created, doing the following:

- 1) Read Extra focal image
- 2) Read Intra focal image. This image is rotated 180 degrees so that the grid points correspond
- 3) Subtract dark (if necessary)
- 4) Apply a softening filter (if necessary). May be applied several times for increased blurring/noise reduction.
- 5) Apply a threshold to obtain a binary image. The threshold level is adjusted in real time so as to have the required number of patches (21)
- 6) Detect the peak within each patch and sort the peaks
- 7) Write peak coordinates to a file

Figure 9 shows an image of the screen. Each action can be addressed separately via the File menu, except action 5, which is done interactively by the aid of slides. They can also be addressed in two groups via buttons: "DoAll" groups actions 1-4 and "Finish" groups actions 6 and 7. Additional filtering can be applied if necessary during the search for threshold. The filtered images are shown on the left and the threshold images are shown on the right. The number of patches found each time a new threshold level is set is printed in the IDL window. **This number should be 21.** Threshold level is in % of peak pixel intensity. Figure 9 shows the screen image when appropriate thresholds have been set, just before pushing the "Finish" button. Notice that although the hole in the BSM mirror blocks most of the Hartmann hole second from the top in the middle column, enough signal is received to define a patch at that point.

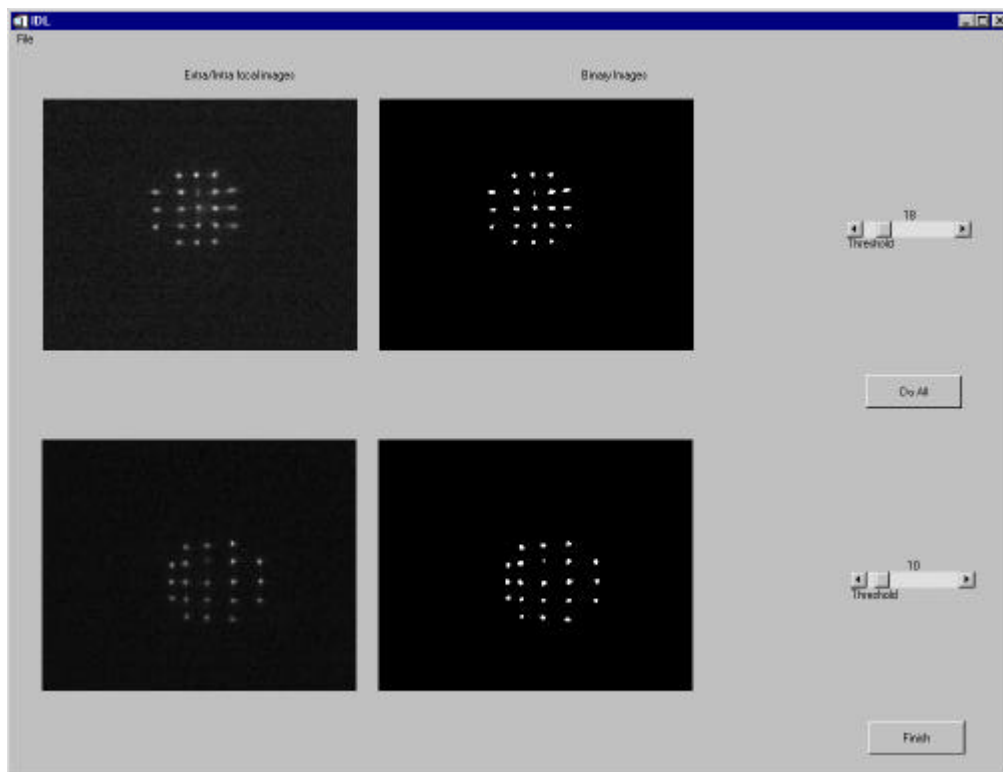


Figure 9. Screen shot of the IDL program for detection and sorting of Hartmann points.

## 5.2. Hartmann data reduction

The data file is imported into an XL file (Current version TraitImagHartTes32.xls) where it occupies a spreadsheet named typically "STM\_PLW\_E" for "Dtool diode E in PLW focal plane of the STM model". The XL file treats the data in two principal sheets:

### 5.2.1. Transverse aberrations: "HartNew"

The Hartmann test allows determination of the transverse aberrations of a system. These are habitually presented in the form of spot diagrams, and correspond to the first derivatives of the system wavefront. Determination of transverse aberrations is effectuated in the spreadsheet named "HartNew" and corresponds to the following main operations:

- Fetch peak coordinate data, units of pixels
- Centre and calculate coordinates in mm. Coordinate axes, labelled Z and Y, are oriented according to SPIRE convention.
- Calculate Z and Y ray slopes as the sum of corresponding extra and intra focal coordinates, divided by the distance between extra and intra focal image planes.
- From slopes, calculate the relative pupil coordinates of each grid point. This is compared with pupil coordinates measured from the photograph of Fig. 2, see Fig. 3.c.
- Calculate theoretical focus coordinates of the rays as they pass through the theoretical focal plane. This equals half the difference of corresponding extra and intra focal coordinates. Plotted in an X-Y plot, this gives the spot diagram to be compared with the theoretical spot diagrams produced by a raytracing program.
- Calculate through-focus spot diagrams by combining theoretical focus coordinates and slope values. Five focal positions are calculated and plotted, with adjustable defocus offset and defocus step.

If the parameter DetFlag = 0, then the spot diagrams are scaled to correspond to the F/8.68 telescope focus. If DetFlag = 1, then the scale corresponds to the F/5 instrument focus.

### 5.2.2. Wavefront aberrations: "ZernikeFit"

Estimation of wavefront errors from transverse aberrations can be done by two methods: Integration [Malacara, *Optical shop testing 2nd ed*, p. 385 (1992)] or by least squares fitting of Zernike polynomials [R. CUBLAICHINI, JOSA 69, p. 972 (1979)]. The latter, developed for adaptive optics (AO) and referred to as the modal approach, was adapted here because of its relative simplicity of implementation and the usefulness of its output in terms of Zernike coefficients.

By this method, the actual transverse aberrations are compared with synthetic aberrations calculated from polynomial functions representing derivatives of the Zernike polynomials and a set of estimated Zernike coefficients. The estimate is improved by damped least squares optimization until the difference between transverse aberrations is minimized.

The following operations are included in the spreadsheet "ZernikeFit":

- Fetch the theoretical-focus ray coordinates from the "HartNew" sheet
- Calculate ray coordinates according to a list of Zernike coefficients using functional representations of the derivatives of the Zernike polynomials (defined in the "Macro" sheet)
- Calculate the RMS of the difference between actual and calculated ray coordinates,
- Using the "Solver" routine (a powerful least squares algorithm built in to EXCEL), the Zernike coefficients are optimized to give minimum RMS difference
- Reconstruct the wavefront using the original (non-derivative) Zernike polynomials (functional forms given in "Macros" sheet) on a high-resolution map. The calculations for this map are done in the sheet "WFmap".

The 14 Zernike modes included in our calculations are defined in Table 2 in their cartesian representation. This is equivalent to the more common radial representation, but makes differentiation easier. The first derivatives are also included, as well as the factor by which the Zernike coefficients are multiplied to give the WFE RMS contribution for each polynomial. Since Zernike polynomials are orthogonal, the RMS error of the reconstructed wavefront equals the RSS of the RMS coefficients.

Table 2. Definition of Zernike polynomials and their derivatives used in our calculations.

No	Name	RMS factor	Wavefront W	X differential $\frac{\partial W}{\partial x}$	Y differential $\frac{\partial W}{\partial y}$
1	TiltX	$1/\sqrt{4} = 0.50$	x	1	0
2	TiltY	$1/\sqrt{4} = 0.50$	y	0	1
3	Focus	$1/\sqrt{3} = 0.58$	$-1+2y^2+2x^2$	4x	4y
4	AstX	$1/\sqrt{6} = 0.41$	$y^2-x^2$	-2x	2y
5	AstY	$1/\sqrt{6} = 0.41$	2xy	2y	2x
6	ComaX	$1/\sqrt{8} = 0.35$	$-2x+3xy^2+3x^3$	$-2+3y^2+9x^2$	6xy
7	ComaY	$1/\sqrt{8} = 0.35$	$-2y+3x^2y+3y^3$	6xy	$-2+3x^2+9y^2$
8	Sph	$1/\sqrt{5} = 0.45$	$1-6y^2-6x^2+6y^4+12x^2y^2+6x^4$	$-12x+24xy^2+24x^3$	$-12y+24x^2y+24y^3$
9	Tri5X	$1/\sqrt{8} = 0.35$	$3xy^2-x^3$	$3y^2-3x^2$	6xy
10	Tri5Y	$1/\sqrt{8} = 0.35$	$y^3-3x^2y$	-6xy	$3y^2-3x^2$
11	Ast5X	$1/\sqrt{10} = 0.32$	$-6xy+8xy^3+8x^3y$	$-6y+8y^3+24x^2y$	$-6x+24xy^2+8x^3$
12	Ast5Y	$1/\sqrt{10} = 0.32$	$-3y^2+3x^2+4y^4-4x^4$	$6x-16x^3$	$-6y+16y^3$
13	Coma5X	$1/\sqrt{12} = 0.29$	$3x-12xy^2-12x^3+10xy^4+20x^3y^2+10x^5$	$3-12y^2-36x^2+10y^4+60x^2y^2+50x^4$	-24xy
14	Coma5Y	$1/\sqrt{12} = 0.29$	$3y-12x^2y-12y^3+10x^4y+20x^2y^3+10y^5$	-24xy	$3-12x^2-36y^2+10x^4+60x^2y^2+50y^4$

## 6. Results

For the STM photometer, only two points (of five foreseen: centre and four corners) were measured by the Hartmann test. The results from these tests have allowed the data reduction to be tested and adapted to real measurement data, and to draw some conclusions regarding the optical quality of the STM.

### 6.1. Reference system

To compare the results obtained by the Hartmann test with the optical model, a new raytracing model (BolPhot155d\_InstrOnly) has been made, replicating the conditions of the test setup:

- The telescope is removed: the test only concerns the instrument optical train
- The curved input focal plane is replaced by a flat input surface, coinciding with the telescope focal surface at the centre of the Photometer FOV and perpendicular to the gut ray: this corresponds to applying only transverse adjustments to the Hartmann lunette as described above.

Figure 10 shows through-focus spot diagrams produced using this model, corresponding to field points E, B, and A. Spots for points C and D are mirror images of those for B and A, respectively. The spot diagrams are produced using 21 rays on a rectangular grid in the pupil, replicating approximately the distribution of rays used in the Hartmann test. The plane object surface coincides approximately with the telescope image surface in points E and B, but in point A, a defocus of about 9mm is introduced. This corresponds to a defocus of 3mm in the instrument focal plane, as can be observed in Figure 10.

NB: When Hartmann tests are to be made on point A during PFM tests, it may be necessary to correct for this defocus to avoid overlapping Hartmann spots.



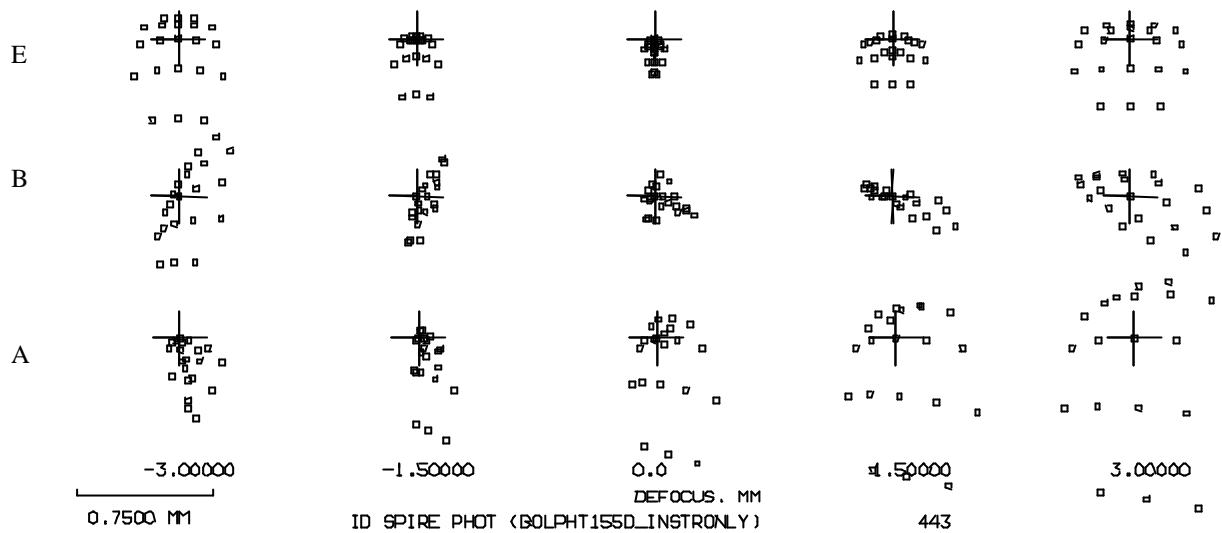


Figure 10. Theoretical through-focus spot diagrams for field points E (upper row), B (middle row), and A (lower row) using the model BolPht155d\_InstrOnly in which the instrument object surface is plane. The five columns correspond to moving the SPIRE detector plane axially in steps of 1.5mm. Positive defocus is upstream of the theoretical image plane, ie before the detector surface.

Table 3 lists Zernike coefficients obtained by ratracing for these field points. Signs and order of the coefficients have been corrected to be in agreement with signs and order used in the Hartmann test calculations. The large focus coefficient (Z3) for field point A reflects the departure from the curved image surface. Axial defocus is calculated from the Z3 coefficient by the expression:

$$\Delta = -16 F\#^2 Z3$$

ie, 0.375 Z3 at F/5 and 1.205 Z3 at F/8,68, when  $\Delta$  is in mm and Z3 is in  $\mu\text{m}$ .

Table 3. Theoretical Zernike coefficients in  $\mu\text{m}$  for points E, B, and A for the model BolPht155d\_InstrOnly in which the instrument object surface is plane.

Zname	Number	SynoZ	InstrOnly_E	InstrOnly_B	InstrOnly_A
			<i>BolPht155d</i>	<i>BolPht155d</i>	<i>BolPht155d</i>
cTiltX	Z1	ZS2	5.02	1.89	9.75
cTiltY	Z2	ZS1	0.00	3.06	3.21
cFocus	Z3	ZS3	-0.32	-0.77	-8.22
cAstX	Z4	ZS4	-1.76	-4.56	5.46
cAstY	Z5	ZS5	0.00	-4.91	-0.48
cComaX	Z6	ZS7	2.47	0.91	4.82
cComaY	Z7	ZS6	0.00	1.53	1.60
cSph	Z8	ZS8	0.24	0.25	0.27
cTri5X	Z9	ZS10	-0.94	-0.47	-1.55
cTri5Y	Z10	ZS9	0.00	-0.34	-0.85
cAst5X	Z11	ZS11	-0.17	-0.14	-0.21
cAst5Y	Z12	ZS12	0.00	0.01	0.02
cComa5X	Z13	ZS14	-0.03	-0.02	-0.04
cComa5Y	Z14	ZS13	0.00	0.00	0.00

## 6.2. Hartmann results

Figure 11 shows through-focus spot diagrams obtained with the Hartmann test for points E and A. The scale is approximately equal to that of Figure 10, but the spots are rotated 90° anticlockwise. A defocus offset of 1mm has been introduced in the case of field point E, see discussion below. While the spots for Point E correspond well with the theoretical spots, some discrepancy is observed for point B. The Zernike analysis quantifies these differences.

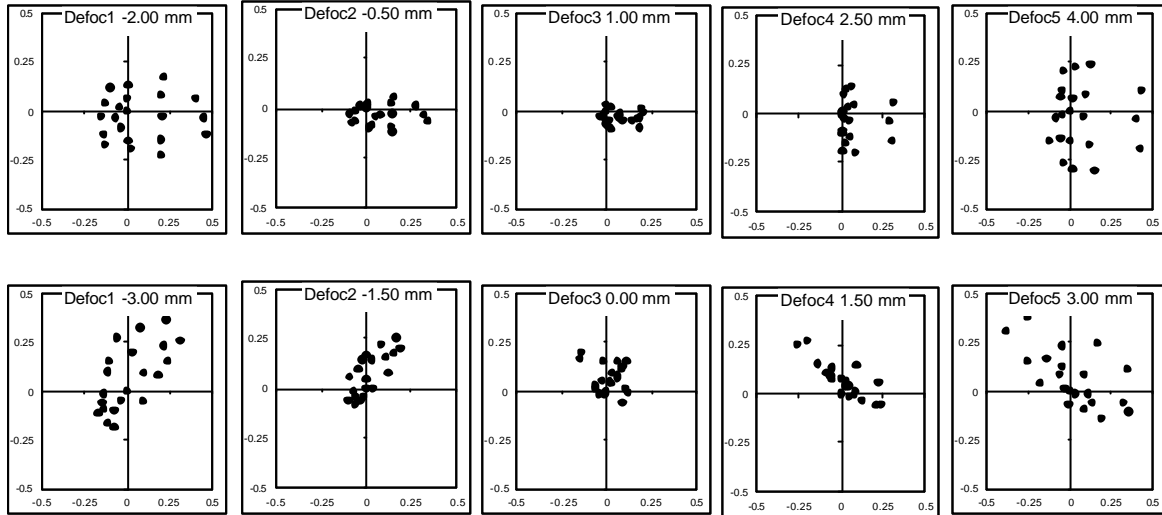


Figure 11. Through-focus spot diagrams obtained from the Hartmann tests for field point E (upper row) and B (lower row). See Figure 10 for explanations.

Table 4 lists Zernike coefficients obtained from the Hartmann test. Comparison with the theoretical coefficients listed in Table 3 indicates differences in most coefficients between 0.15 and 0.45 $\mu\text{m}$ . This is probably representative of the inherent noise level due to cumulative errors in the test method. Although a proper error analysis has not been effectuated, the main error source is expected to be the precision of Hartmann spot coordinate determination. Differences between the theoretical system and the measured results greater than 0.5 $\mu\text{m}$  are also listed in Table 3.

Table 4. Experimentally obtained Zernike coefficients in  $\mu\text{m}$  for points E and B.

Zname	Number	SynoZ	PhtSTM_E $\mu\text{m}$ WFE	PhtSTM_B $\mu\text{m}$ WFE	Difference E $\mu\text{m}$ WFE	Difference B $\mu\text{m}$ WFE
cTiltX	Z1	ZS2	4.48	1.58		
cTiltY	Z2	ZS1	-3.21	5.28		
cFocus	Z3	ZS3	-2.51	-0.34	-2.19	
cAstX	Z4	ZS4	2.52	-1.36	+4.28	+3.20
cAstY	Z5	ZS5	-0.15	-5.59		-0.68
cComaX	Z6	ZS7	2.64	0.55		
cComaY	Z7	ZS6	-0.18	1.93		
cSph	Z8	ZS8	0.66	1.17		+0.92
cTri5X	Z9	ZS10	-1.35	-0.85		
cTri5Y	Z10	ZS9	0.30	-0.57		
cAst5X	Z11	ZS11	0.22	-0.21		
cAst5Y	Z12	ZS12	-0.73	-0.15	-0.73	
cComa5X	Z13	ZS14	0.19	-0.18		
cComa5Y	Z14	ZS13	0.22	0.26		

## 7. Discussion

The 2.19 $\mu\text{m}$  difference in Z3 for point E, corresponding to a defocus of 0.82mm at F/5, is responsible for the focal shift observed in the spot diagrams. This error corresponds to an RMS WFE of  $Z3/\sqrt{3} = 1.26\mu\text{m}$ , in good agreement with the error budget [RD3] allocation of WFE RMS = 1.15 $\mu\text{m}$  if all mirrors had a relative error of  $10^{-3}$  in their radius of curvature. Although test results indicate that some mirrors are worse than this, the overall effect is similar.

The most important difference concerns the Z4 coefficient, where both points suffer from an increase of about 4 $\mu\text{m}$ , corresponding to  $Z4/\sqrt{6} = 1.63\mu\text{m}$  WFE RMS. This error is likely to have three main sources:

- Astigmatic deformation of some mirrors, probably due to stress relaxation
- Differential errors between the two radii of toroidal surfaces
- The definition error of CM3

The definition error of CM3 has been shown [RD4] to be dominated by  $Z4 = 6\mu\text{m}$  (AstX) and  $Z5 = 21\mu\text{m}$  (AstY) on the mirror surface, ie twice as much on a reflected wavefront. However, since CM3 is close to the focal plane, the effect on the image quality is reduced to about 0.5% of this, hence insignificant in this context. The main contribution is probably from astigmatic surface deformations. The error budget [RD3] allocates 2 $\mu\text{m}$  WFE RMS per mirror (ie 1 $\mu\text{m}$  RMS surface error) for a total budget allocation of 6 $\mu\text{m}$  WFE RMS. The measured wavefront error of 1.63 $\mu\text{m}$  is well within this allocation.

The Coma coefficients show good agreement. Coma, which is not easily generated during surface fabrication, is usually an indicator of misalignment errors.

A more compact representation of the Zernike data is given in Table 5. Here, the two terms of non-symmetrical aberrations are root-sum-squared (RSS) to give the total for each term, and each coefficient is multiplied by the corresponding RMS factor (see Table 1). This table therefore shows the contribution to the RMS wavefront error for each term. Total RMS wavefront error at best focus is also shown, as well as corresponding Strehl ratio at 250 $\mu\text{m}$ . The table allows comparison between the theoretical instrument and the as-built instrument.

The final WFE of the as-built model can also be compared with the error budget [RD3], which allocates 8.2 $\mu\text{m}$  WFE RMS to the instrument. With a measured WFE RMS of 2.5  $\mu\text{m}$  at field point B, the SPIRE STM is therefore fully acceptable from the point of view of image quality, including focus.

Table 5. Comparison of RMS coefficients, total RMS wavefront error, and corresponding Strehl ratio at 250 $\mu\text{m}$  for the raytracing model and for the as-built STM.

Aberration	InstrOnly_E	InstrOnly_B	PhtSTM_E	PhtSTM_B
Focus	0.18	0.44	1.45	0.20
Astigmatism	0.72	2.74	1.03	2.35
Coma	0.87	0.63	0.94	0.71
SphAb	0.11	0.11	0.29	0.52
Tri5	0.33	0.21	0.49	0.36
Ast5	0.05	0.04	0.24	0.08
Coma5	0.01	0.01	0.08	0.09
<b>WFE RMS</b>	<b>1.20</b>	<b>2.85</b>	<b>2.10</b>	<b>2.54</b>
<b>Strehl 250um</b>	<b>0.999</b>	<b>0.995</b>	<b>0.997</b>	<b>0.996</b>